J. Radiat. Res., 53, 202–210 (2012)

Combination of Radiotherapy and Adenovirus-Mediated *p53* Gene Therapy for MDM2-Overexpressing Hepatocellular Carcinoma

Woong Sub KOOM[1], Soo-Yeon PARK[2], Wonwoo KIM[2], Minjung KIM[2], Ji-Seong KIM[2], Hyunki KIM[3], Il-Kyu CHOI[4], Chae-Ok YUN[2,4] and Jinsil SEONG[1]*

p53/MDM2/Radiotherapy/Adenovirus/Gene therapy.

The *p53* gene plays a determinant role in radiation-induced cell death and its protein product is negatively regulated by MDM2. We investigated whether adenovirus-mediated modified *p53* gene transfer, which blocks p53-MDM2 binding, is effective for radiation-induced cell death in hepatocellular carcinoma (HCC) at different MDM2 cellular levels. Human hepatocellular carcinoma cell lines expressing MDM2 at low levels (Huh7) and high levels (SK-Hep1) were used. Ad-p53 and Ad-p53vp are replication-deficient adenoviral vectors containing human wild-type or modified p53, respectively. The anti-tumor effect was highest for Ad-p53 + radiotherapy (RT) in the low-level MDM2 cells, whereas this effect was highest for Ad-p53vp + RT in the MDM2-overexpressing cells. In Huh-7 cells, Ad-p53 + RT decreased cell viability (32%) *in vitro* and inhibited tumor growth (enhancement factor, 1.86) *in vivo*. Additionally, p21 expression and apoptosis were increased. In contrast, in SK-Hep1 cells, Ad-p53vp + RT showed decreased cell viability (51%) *in vitro* and inhibition of tumor growth (enhancement factor, 3.07) *in vivo*. Caspase-3 expression and apoptosis were also increased. Adenovirus-expressing modified p53, which blocks p53-MDM2 binding, was effective in killing tumor cells overexpressing MDM2. Furthermore, the combination strategy for disruption of the p53-MDM2 interaction with RT demonstrated enhanced anti-tumor effects both *in vitro* and *in vivo*.

INTRODUCTION

The advanced stage hepatocellular carcinoma (HCC) in Barcelona-Clinic Liver Cancer (BCLC) classification involves a wide spectrum of disease involving portal vein invasion, metastases, and performance 0–2.[1,2] While sorafenib is known as a standard of treatment, its effect seems insufficient for the patients with locally advanced disease, who requires a significant cytoreduction.

In the past, radiotherapy (RT) has played a minor role in the treatment of HCC due to low radiation tolerance of the liver.[3] With recent advances in RT technology a substantial dose of radiation can be delivered to tumors avoiding normal sensitive organ.[4,5] A significant local tumor control as well as possible survival impact has been reported, drawing increased attention as a useful modality in locally advanced HCC. However, tumor response to RT still remains to be improved. A clue to increasing intrinsic radiosensitivity of HCC is *p53* gene mutation, which has been found in many tumor types including HCC.[6]

The *p53* gene plays an essential role in the cellular response to DNA damaging agents, including RT. RT has been shown to promote p53 protein expression posttranslationally, leading to either cell cycle arrest or apoptosis through p53's function as a transcriptional regulator of p53-responsive genes.[7] The MDM2 protein plays a critical role in the regulation of p53 protein stability and function. MDM2 regulates p53 activity through a negative feedback loop:[8] MDM2 directly binds to the p53 transactivation domain,[9] leading to ubiquitination, nuclear export, and nuclear and cytoplasmic proteasomal degradation of p53.[10] High levels of MDM2 inhibit p53-mediated tumor suppressing activity through p53 inactivation. The disruption of the p53-MDM2 interaction has been reported to induce p53 stabilization and transcriptional activation, resulting in cell cycle arrest or apoptosis.[11] Additionally, MDM2 binding to p53 might limit the effectiveness of RT. Thus, blocking the p53-MDM2 interaction may increase the functional p53

*Corresponding author: Phone: +82-2-2228-8111,
Fax: +82-2-312-9033,
E-mail: jsseong@yuhs.ac
[1]Department of Radiation Oncology, [2]Brain Korea 21 Project for Medical Sciences, Institute for Cancer Research, [3]Department of Pathology, Institute for Cancer Research, Yonsei Cancer Center, Yonsei University College of Medicine, Seoul 120-752, Republic of Korea; [4]Graduate Program for Nanomedical Science, Yonsei University, Seoul 120-749, Republic of Korea.
Conflict of Interest Statement: There is no conflict of interest in connection with this work.
doi:10.1269/jrr.11110

activation after RT, thereby enhancing the therapeutic effectiveness of RT. We focused on modification of the p53 transactivation domain, which contains an MDM2 binding site, to block the MDM2 negative feedback loop. Our hypothesis was that modified *p53* gene transfer using an adenoviral vector would enhance the cellular response to RT by inhibiting the p53-MDM2 interaction.

In the present study, we investigated whether adenovirus-mediated modified *p53* gene transfer is effective for RT-induced cell death at different MDM2 cellular levels and whether apoptosis or cell cycle arrest is the underlying mechanism in both *in vitro* and *in vivo* human HCC models.

MATERIALS AND METHODS

Cell lines and culture

The human HCC cell lines Huh-7 (mutant p53, low MDM2 expression) and SK-Hep1 (wild-type p53, high MDM2 expression) were obtained from the American Type Culture Collection (ATCC, Manassas, VA, USA). Cells were cultured in Dulbecco's modified Eagle's medium (DMEM) supplemented with 10% fetal bovine serum (FBS; Gibco-BRL, Grand Island, NY, USA), 2 mmol/L glutamine, 50 units/ml penicillin, and 50 μg/ml streptomycin (Gibco-BRL) at 37°C in an atmosphere of 5% CO_2.

Animal studies

In vivo tumor experiments were performed using 6- to 8-week-old male nude mice (BALB/c-nu) purchased from Charles River Korea (Seoul, South Korea). All mice were maintained in a laminar air flow cabinet under specific pathogen-free conditions. All facilities were approved by the Association of Assessment and Accreditation of Laboratory Animal Care (AAALAC), and all animal experiments were performed under the institutional guidelines established by the Animal Core Facility at Yonsei University College of Medicine.

Adenoviral vectors expressing p53 or p53vp gene and experimental groups

Replication-defective adenoviral vectors were provided by Chae-Ok Yun at Yonsei Cancer Center. We used two therapeutic genes, wild-type p53 and modified p53 (p53vp). To generate p53vp, which avoids the negative feedback loop with MDM2, the p53 transactivation domain (containing the MDM2 binding site) was replaced with herpes simplex virus vp16. Both genes were inserted into the E1 region of the adenovirus genome to generate replication-deficient adenoviral vectors Ad-p53 or Ad-p53vp containing human wild-type p53 or modified p53, respectively (Fig. 1). To compare single with combination therapy, experimental groups were categorized into six groups as follows: control, RT alone, Ad-p53 alone, Ad-p53 + RT, Ad-p53vp alone, and Ad-p53vp + RT.

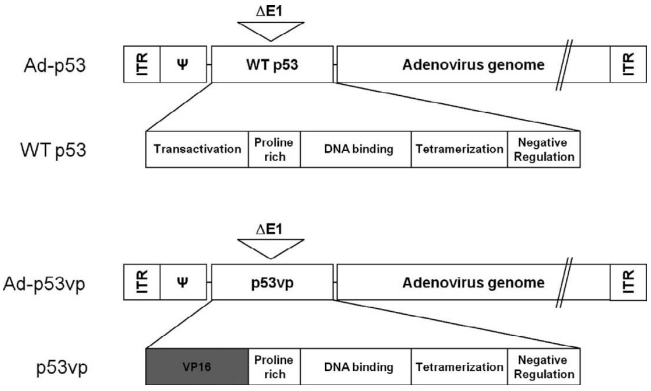

Fig. 1. Schematic representation of the adenoviral vectors. Replication-deficient adenovirus has the whole E1 region deleted. Wild-type p53 and p53vp is inserted into the E1 region. Δ E1 = deletion of the E1 gene; ITR = inverted terminal repeat; Ψ = packaging signal.

Cell viability assay (MTT assay)

The effectiveness of the combined treatment of Ad-p53 or Ad-p53vp and RT was assessed using the MTT assay. One day before treatment, 10^4 cells were seeded onto 48-well plates. Cells were infected at a multiplicity of infection (MOI) of 10 with Ad-p53 or Ad-p53vp for 24 h, and then exposed to 10 Gy of RT using a Siemens Primart 6 MV linear accelerator (Siemens Medical Solutions, Concord, CA, USA). Three days after treatment, the absorbance at 540 nm was determined using a microplate reader (SpectraMax 340; Molecular Devices, Sunnyvale, CA, USA). All assays were performed in triplicate.

Western blot analysis

Following treatment, cells were harvested at 4, 8, 24, and 48 h, and then were lysed with cell lysis buffer (Cell Signaling Technology, Beverly, MA, USA) for 30 min on ice. The protein concentration of cell lysates was determined using the Bio-Rad Protein Assay kit (Bio-Rad Laboratories, Hercules, CA, USA). The following antibodies were used: anti-p53 (Santa Cruz Biotech, Santa Cruz, CA, USA), anti-p21 (Santa Cruz Biotechnology, Santa Cruz, CA, USA), anti-MDM2 (Santa Cruz Biotechnology), anti-cleaved caspase-3 (Abcam, Cambridge, UK), and anti-β-actin (Sigma). Immunoreactive proteins were detected with secondary antibodies and visualized using an enhanced chemiluminescence detection system (Amersham Bioscience, Piscataway, NJ, USA).

Antitumor effect in vivo

Tumor cells (1×10^7 cells of Huh7 or SK-Hep1) were injected into the right thighs of male nude mice. When the tumor size reached a mean diameter of 7.5–8 mm, three mice were randomly assigned to each of the six groups. For the phosphate-buffered saline (PBS) alone or adenovirus alone group, adenovirus [Ad-p53 or Ad-p53vp at 5×10^{10}

virus particles (VP)] was administered intratumorally three times every other day (day 0, 2, and 4) in a volume of 50 μl diluted in PBS. For the RT alone or combination group, a RT dose of 10 Gy photon in a single fraction was delivered to the tumor-bearing legs on day 1 using a Siemens Primart 6 MV linear accelerator (Siemens Medical Solutions). For tumor growth delay analysis, tumor measurements at three orthogonal tumor diameters were recorded every 2 days until the tumors grew to >12 mm in mean diameter. The effect of the treatment on tumor growth delay was expressed as the absolute growth delay (AGD), which was defined as the time in days for 8-mm tumors to grow to 12 mm in the treated group minus the mean time for the 8-mm tumors to reach 12 mm in the untreated control group. The enhancement factor (EF) was calculated by dividing the normalized tumor growth delay (NGD) by the AGD. The NGD was defined as the time in days for tumors to grow from 8 to 12 mm in mice treated with the combination treatment minus the time in days for tumors to reach 12 mm in the adenovirus only-treated group.[12)]

Terminal deoxynucleotidyl transferase-mediated dUTP-biotin nick end labeling (TUNEL) assay

Apoptosis levels were analyzed using the TUNEL assay. Tumors were immediately excised and placed in 10% neutral buffered formalin 3 days after treatment as described in the tumor growth delay assay. Tissues were embedded in paraffin blocks and 4-μm sections were cut and stained using the ApopTag staining kit (Millipore Corporation, Billerica, MA, USA). TUNEL-positive cells were scored on coded slides at 400× magnification and were considered apoptotic only when accompanied by apoptotic morphology. To calculate the apoptotic index, 10 fields in non-necrotic areas were selected randomly across each tumor section, and, in each field, apoptotic bodies were expressed as a percentage based on the scoring of 1000 nuclei.

Immunohistochemistry (IHC)

Tumor specimens harvested at 3 days after treatment were fixed in 10% neutral buffered formalin, embedded in paraffin wax, and cut into serial sections of 4-μm thickness. Tissue sections were then deparaffinized in xylene (3 × 10 min) and rehydrated through a series of graded alcohols (100%, 95%, 90%, 80%, and 70%). Immunohistochemical staining for p53, MDM2, p21, and cleaved caspase-3 protein was performed using anti-p53 (Ab-5; 1/100 dilution; Calbiochem/EMD Biosciences, Darmstadt, Germany), anti-MDM2 (Ab-5; 1/100 dilution; Calbiochem/EMD Biosciences), anti-p21 (Ab-5; 1/100 dilution; Calbiochem/EMD Biosciences), and anti-cleaved caspase-3 (13S-5; 1/100 dilution; Santa Cruz Biotechnology), respectively. Sections were visualized using the Envision-HRP kit (K5007, Dakocytomation, Glostrup, Denmark). The peroxidase binding sites were detected by staining with diaminobenzidine (DAB; DAKO A/S, Glostrup, Denmark), and the sections were finally counterstained with Mayer's hematoxylin and observed under a light microscope.

Statistical analysis

Data were expressed as mean ± standard error of the mean. Statistical comparisons between experimental groups were performed using the Mann–Whitney *U* test. Statistical significance was defined as $P < 0.05$.

RESULTS

Ad-p53vp is functional and expresss p53 protein in MDM2-overexpressing cell lines

The endogenous expression of p53 and MDM2 was first determined in Huh7 and SK-Hep1 cells by Western blotting. p53 was highly expressed in Huh7 but minimally expressed in SK-Hep1 cells (Fig. 2A, lane 1). A high MDM2 level was observed only in SK-Hep1 but not in Huh7 cells. To characterize the gene transfer activity of Ad-p53 and Ad-p53vp, the effect of Ad-p53 and Ad-p53vp on p53 and MDM2 levels was determined by Western blotting. Huh7 (low MDM2 levels) and SK-Hep1 cells (high MDM2 levels) were infected with Ad-p53 and Ad-p53vp at an MOI of 10 each. At 12, 24, and 48 h, cells were harvested and lysates were immunoblotted for p53 and MDM2 (Fig. 2A). In Huh7 cells, the p53 level was elevated in a time-dependent manner, peaking at 24 h. Additionally, MDM2 expression was also up-regulated as p53 expression increased. This pattern was similar between Ad-p53 and Ad-p53vp. In contrast, p53 levels in SK-Hep1 cells were significantly increased after treatment with Ad-p53vp compared with Ad-p53. MDM2 levels were also significantly increased after Ad-p53vp treatment. This result indicated that adenovirus expressing modified p53 is functional in MDM2-overexpressing cell lines and escapes the negative feedback of MDM2.

Combination of Ad-p53 or Ad-p53vp with radiotherapy increases cell death in vitro

The *in vitro* anti-tumor effects of combined treatment were evaluated using the MTT assay 3 days after treatment. Before examining the cytotoxic effect of the combination treatment, Ad-p53 or Ad-p53vp as a single agent was evaluated at different MOI (Fig. 2B). In Huh7 cells, the cell viability was decreased in a dose-dependent manner and the levels were comparable in the two viruses. In contrast, Ad-p53 did not show a dose-dependent effect on cell death in SK-Hep1 cells. The level of cell viability in Ad-p53vp was decreased in a dose-dependent manner even in MDM2-overexpressing SK-Hep1 cells.

Next, to test if exogenous wild-type or modified *p53* gene would improve the cell death effect of RT at different MDM2 levels, Huh7 and SK-Hep1 cells were infected with Ad-p53 and Ad-p53vp at an MOI of 10 each, and were then

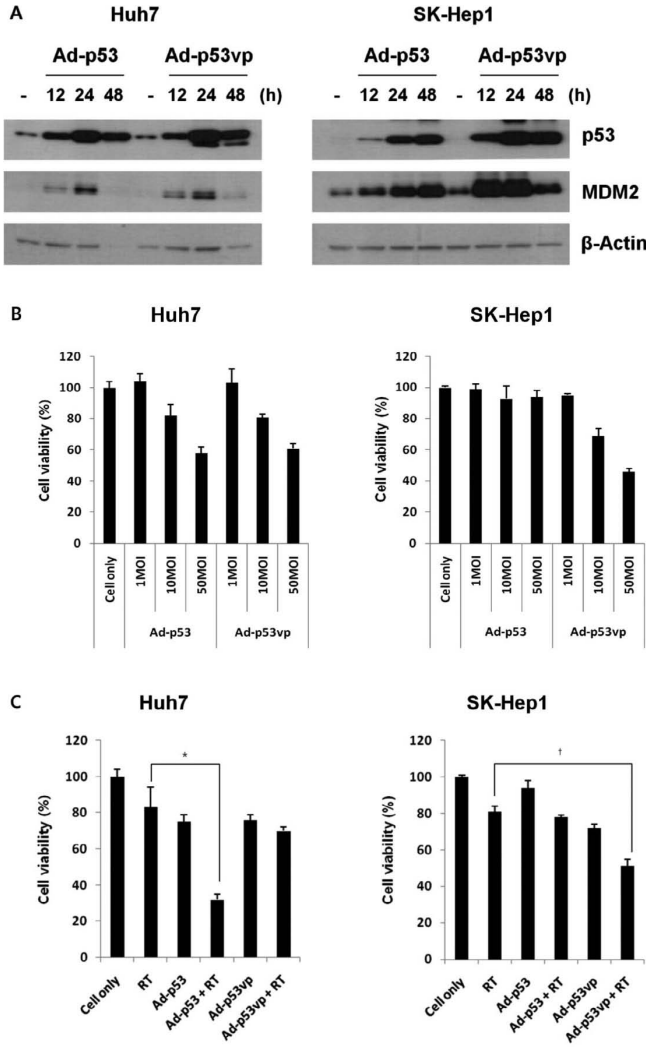

Fig 2. Basal level of p53 and MDM2 in Huh7 and SK-Hep1 cells and Cell-killing effect of the combination of Ad-p53 or Ad-p53vp with RT. (A) Western blot analysis of p53 and MDM2 in Huh7 and SK-Hep1 cells after treatment with Ad-p53 or Ad-p53vp; (B) Cell-killing effect of Ad-p53 and Ad-p53vp according to multiplicity of infection (MOI). (C) Cell-killing effect of the combination of Ad-p53 or Ad-p53vp with RT. Cell viability was assessed using the MTT [3-(4, 5-dimethylthiazol-2yl)-2, 5-diphenyltetrazolium bromide] assay 3 days after RT and is expressed as a percentage of untreated controls ± s.e.m. *P = 0.01 (Huh7); †P = 0.02 (SK-Hep1).

treated with 10 Gy of RT in 24 h. Figure 2C illustrates the results of the six experimental groups. In Huh7 cells, RT resulted in approximately 20% cell death. Ad-p53 alone also demonstrated a similar effect with 25% cell death. Significantly, increased cell death was observed in the combination treatment of Ad-p53 and RT with about 70% cell death. Although Ad-p53vp was comparable to Ad-p53 as a single agent, the combination of Ad-p53vp and RT resulted in a minimal increase in cell death comparing with RT alone. In contrast, in SK-Hep1 cells, Ad-p53vp as a single agent was more effective with about 30% cell death compared with Ad-p53 at 5% cell death. RT resulted in approximately 20% cell death, also. The effect of the combination of Ad-p53 and RT was similar to that of RT alone. However, the combination treatment of RT and Ad-p53vp significantly increased cytotoxicity (50% cell death). These results indicated that the cell killing effect induced by exogenous p53 depends on the MDM2 level, and modified p53 is effective in overcoming p53 degradation by MDM2. Moreover, RT following transfer of exogenous p53 or p53vp results in an enhanced cell death effect.

p53 downstream transcriptional targets are activated in the combination treatment of Ad-p53 or Ad-p53vp with radiation

To test whether Ad-p53 or Ad-p53vp could up-regulate p53 downstream proteins and whether combination treatment with RT would enhance the levels of these proteins at different MDM2 levels, we performed Western blotting for p53, MDM2, p21, and caspase-3 at different time points (4, 8, 24, and 48 h) (Fig. 3). In Huh7 cells, both Ad-p53 and Ad-p53vp increased p53 accumulation and MDM2 accumulation was increased by p53 transcriptional activity. p21 and caspase-3 levels were significantly elevated with Ad-p53 compared with Ad-p53vp at 24 h (Fig. 3, lane 3 vs. lane 5 in Huh7). In the combination treatment, p21 was not increased after RT with Ad-p53 or Ad-p53vp (Fig. 3, lane 3 vs. lane 4 and lane 5 vs. lane 6 in Huh7). The caspase-3 levels between Ad-p53vp alone and Ad-p53vp with RT were similar (Fig. 3, lane 5 vs. lane 6 in Huh7). However, we found a prominent increase of caspase-3 in Ad-p53 with RT at 24 h (Fig. 3, lane 3 vs. lane 4 in Huh7). In Sk-Hep1 cells, Ad-p53vp induced elevated levels of p53, p21, and caspase-3 compared with Ad-p53 until 48 h, although the level of MDM2 was also increased more with Ad-p53vp than with Ad-p53 (Fig. 3, lane 3 vs. lane 5 in SK-Hep1). When RT was administered with adenovirus, the caspase-3 levels were slightly increased in Ad-p53 plus RT (Fig. 3, lane 3 vs. lane 4 in SK-Hep1) but similar in Ad-p53 plus RT (Fig. 3, lane 5 vs. lane 6 in SK-Hep1). However, p21 accumulation was most pronounced in Ad-p53vp and RT at 48 h (Fig. 3, lane 5 vs. lane 6 in SK-Hep1). These results showed that the combined treatment of Ad-p53 or Ad-p53vp with RT increased the accumulation of p53 downstream proteins such as p21 and caspase-3 in the different MDM2 level. A prominent accumulation of caspase-3 and p21 in the comparison with other treatment group was observed in Ad-p53 with RT for low MDM2 level and in Ad-p53vp with RT for high MDM2 level, respectively.

Combination of Ad-p53 or Ad-p53vp with radiation enhances anti-tumor effects in vivo

The antitumor effects of the combination treatment were

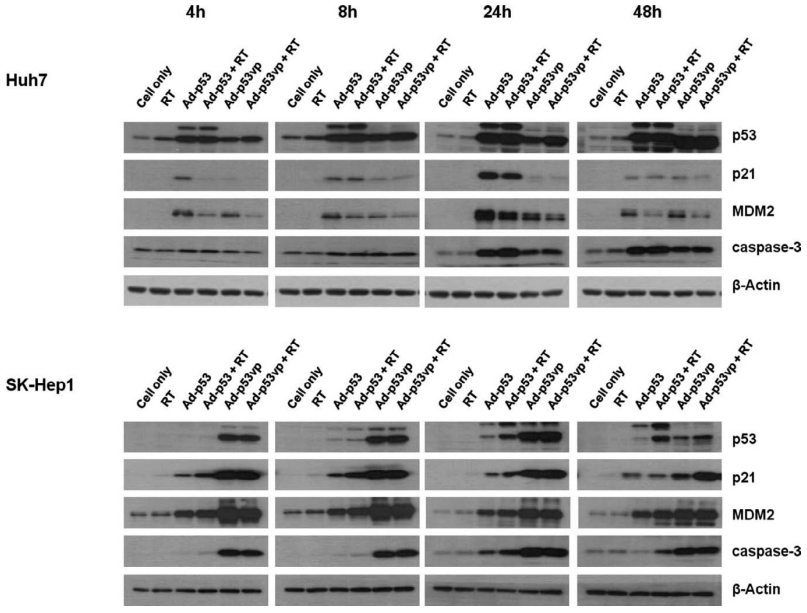

Fig. 3. Western blot analysis of the expression of p53 downstream molecules in a time-dependent manner. p53, MDM2, p21, and cleaved caspase-3 protein were analyzed in Huh7 and SK-Hep1 cells. Each cell line was infected at a MOI of 10 with Ad-p53 or Ad-p53vp, and then treated with 10 Gy of RT.

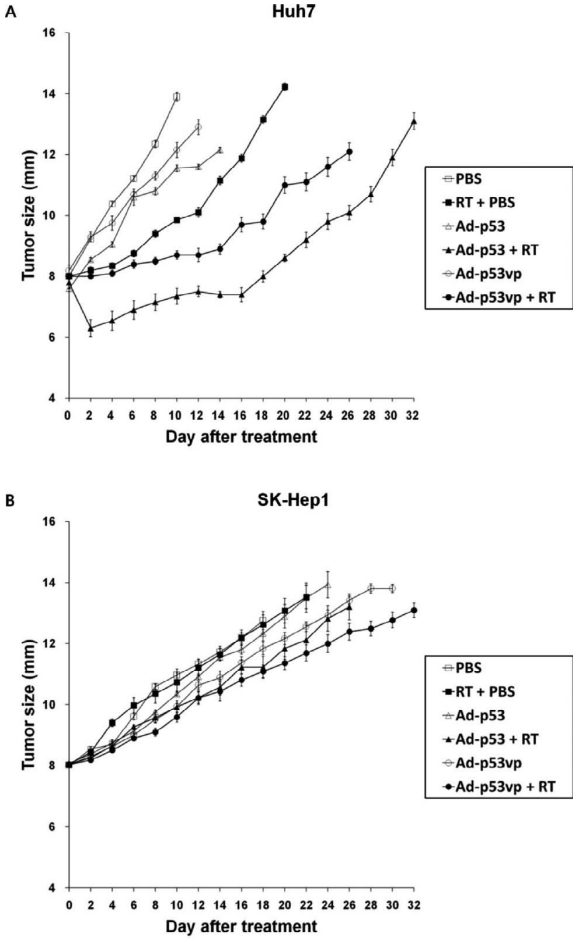

determined using the tumor growth delay assay (Fig. 4A). In the Huh7 xenograft tumor model, a substantial tumor volume growth delay for the combination of Ad-p53 or Ad-p53vp with RT was observed compared with the corresponding treatment groups, including Ad-p53 alone, Ad-p53vp, as well as RT alone. The enhancement factor for the combination treatment of Ad-p53 and RT or Ad-p53vp and RT vs. RT alone was 1.86 and 1.79, respectively (Table 1). Although the absolute difference in tumor growth delay was not remarkable among experimental groups for SK-Hep1 xenograft tumors, the combined treatment demonstrated increased tumor growth inhibition (Fig. 4B). Significantly, the strongest tumor growth delay was observed in the combination of Ad-p53vp with RT compared with radiation alone, resulting in an EF of 3.07 (Table 1).

Apoptosis in the combination of Ad-p53 or Ad-p53vp with RT was verified using TUNEL staining (Fig. 5A) and the results were in accordance with tumor growth delay. In Huh-7 tumor tissue, Ad-p53 with RT showed the highest apoptotic index (24%) (Fig. 5B). In contrast, in SK-Hep1 tumor tissue, the number of TUNEL-positive cells was

Fig. 4. Tumor growth delay in xenograft tumor models. (A) Huh7 and (B) SK-Hep1 cells were treated with phosphate-buffered saline (PBS; □), radiation (RT; ■), Ad-p53 (△), Ad-p53 + RT (▲), Ad-p53vp (○) and Ad-p53vp + RT (●). Adenovirus (5×10^{10}) virus particles (VP) were administered on days 0, 2, and 4. RT (10 Gy) was performed on day 1 in the combined treatment. Data indicate the mean ± s.e.m. of tumor size.

Table 1. Effect of Ad-p53 or Ad-p53vp on radioresponse for tumor growth delay in Huh7 and SK-Hep1 xenograft tumor models.

	Huh7				SK-Hep1			
	Day*	AGD†	NGD‡	EF§	Day*	AGD†	NGD‡	EF§
PBS	7.2				15.3			
RT + PBS	15.8	8.6			16.6	1.3		
Ad-p53	13.8	6.6			17.3	2		
Ad-p53 + RT	29.8	22.6	16	1.86	20.6	5.3	3.3	2.53
Ad-p53vp	10.4	3.2			19.3	4		
Ad-p53vp + RT	25.8	18.6	15.4	1.79	23.3	8	4	3.07

Abbreviations: Huh7, low levels MDM2; SK-Hep1, high levels MDM2; AGD, absolute growth delay; NGD, normalized tumor growth delay; EF, enhancement factor; PBS, phosphate-buffered saline, FBS, fetal bovine serum; RT, radiotherapy.

* Mean value of days for tumor size from 8 to 12 mm.

† AGD (Absolute growth delay) is defined as the time in days for tumors in the treated groups to grow from 8 to 12 mm minus the time in days for tumors in the untreated control group to reach the same size.

‡ NGD (Normalized tumor growth delay) is defined as the time for tumors in the combination treatment groups to grow from 8 to 12 mm minus the time to reach the same size in mice treated with adenovirus alone.

§ EF (enhancement factor) was calculated as the ratio of NGD in mice in the combination treatment groups to AGD in mice treated by radiation alone.

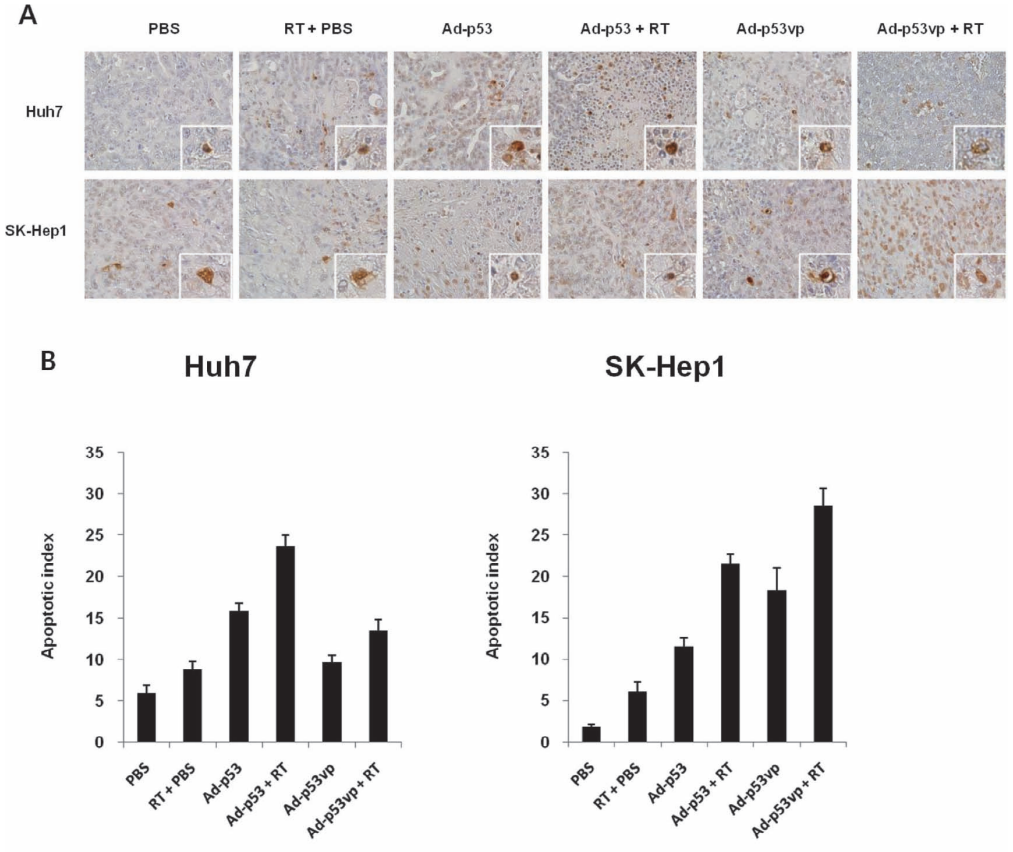

Fig. 5. Apoptosis effect of the combination of Ad-p53 or Ad-p53vp with RT in Huh7 and SK-Hep1 tumor tissues. (a) Detection of apoptosis by TUNEL (terminal deoxynucleotidyl transferase dUTP nick end labeling) assay (×400). Apoptotic cell was demonstrated in right corner box. (b) Apoptotic index as the percent number of apoptotic bodies per 1000 nuclei.

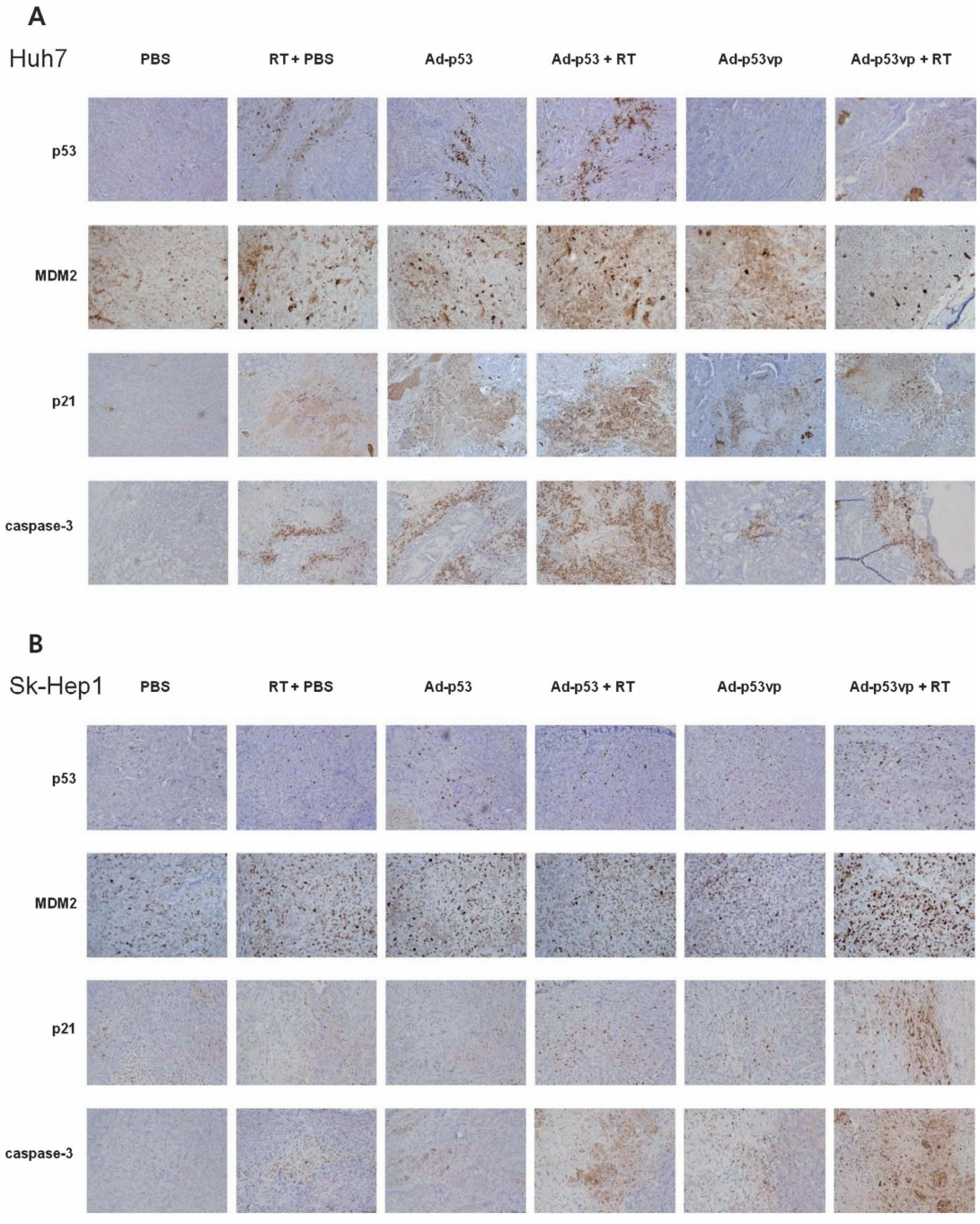

Fig. 6. Immunohistochemical staining for p53 downstream molecules in tumor tissues from Huh7 (a) and SK-Hep1 (b) cells. p53, MDM2, p21, and cleaved caspase-3 were stained (×200).

notably elevated in the combination of Ad-p53vp with RT. Additionally, we performed immunohistochemical staining for p53 downstream molecules, including p21 and caspase-3 (Fig. 6A and B). In Huh-7 tumor tissue, caspase-3 and p21 expression was most prominent in the treatment of Ad-p53 and RT. In contrast, in SK-Hep1 tumor tissue, Ad-p53vp and RT induced most prominent expression of p21 and caspase-3. These results demonstrated that the combination treatment of adenovirus and RT increased expression of p53 downstream molecules depending on the MDM2 level.

DISCUSSION

In the present study, our hypothesis was that modification of the MDM2 binding site in p53 enhances the cell-killing effect of RT by overcoming the negative feedback of MDM2

in cells overexpressing MDM2. Adenovirus-mediated modified *p53* gene transfer with RT showed increased anti-tumor effects in MDM2-overexpressing cells. Conversely, in low-MDM2 expressing cells, wild-type p53 was most effective in combination with RT. Depending on the MDM2 level, p53 downstream molecules, including p21 and caspase-3, were activated. These results underscore the significance of the disruption of the p53-MDM2 interaction as a radiosensitizing strategy.

p53 and its downstream molecules have been demonstrated to be major factors in the response to RT.[13,14] Up-regulated p53 after RT serves as a transcriptional factor to induce expression of downstream p53 molecules. p21 can inactivate the action of cyclin-dependent kinases with consequent cell cycle arrest at the G1 to S phase. Alternatively, several p53-regulated genes induce a protease cascade, leading to activation of caspase-3 and subsequent apoptosis.[15,16] Enhancement of wild-type p53 expression by replication-deficient adenovirus has been shown to increase cytotoxic effects in several cell lines, both *in vitro* and *in vivo*.[17,18] Additionally, the combination of adenovirus-mediated wild-type *p53* gene transfer with RT has been investigated, resulting in enhanced cytotoxicity either via cell cycle arrest or apoptosis.[19,20] p53 radiosensitivity may depend on the restoration of functional p53. However, these enhanced effects are less conclusive in tumor cells with nonfunctional p53 protein even with the combined treatment of exogenous p53 over-expression with RT.[21] MDM2 has been demonstrated to bind and negatively regulate p53 transcriptional function in several cancer types.[22,23] Following treatment with DNA damage agents, including RT, MDM2 is one of several downstream genes activated by p53. In turn, up-regulated MDM2 inhibits p53 function, which creates an autoregulatory feedback loop, resulting in limitations for the efficacy of DNA-damaging treatment.[24,25]

p53 consists of an N-terminal transactivation domain, a proline-rich domain, a DNA-binding core domain, a C-terminal tetramerization domain, and a regulatory domain. MDM2 binds to the N-terminal transactivation domain of p53 with residues 19, 23, and 26 in p53 being critical for this interaction,[26] leading to ubiquitination, nuclear export, and nuclear and cytoplasmic proteasomal degradation of p53.[10,27-29] Therefore, blocking the p53-MDM2 interaction will be an important target to maintain functional p53 levels after RT.[30,31] Therapeutic approaches targeting the disruption of the p53-MDM2 interaction have been developed resulting in cell cycle arrest or p53-dependent apoptosis.[11] In the current study, we focused on the MDM2 binding site in p53. The p53 transactivation domain was replaced by herpes simplex viral vp16 to prevent MDM2 binding. In MDM2-overexpressing cells, modified p53 induced increased protein accumulation, including that of p53, p21, and caspase-3 compared with wild-type p53. Furthermore, the cytotoxic effect of modified p53 was increased depending on the MOI compared with wild-type p53. This difference was not prominent in cells with low MDM2 levels.

We investigated the anti-tumor effect of the combined treatment of RT with either wild-type p53 or modified p53 at different MDM2 levels both *in vitro* and *in vivo*. Our hypothesis was that disruption of p53-MDM2 binding could enhance RT sensitivity through the p53 pathway. Enhanced cytotoxicity, apoptosis, and tumor growth delay were observed according to the MDM2 level. At low MDM2 levels, wild-type p53 and RT demonstrated a significantly enhanced anti-tumor effect. However, with MDM2 overexpression, modified p53 with RT enhanced this effect more effectively compared with either agent alone. Additionally, we investigated the molecular mechanisms involved in the enhancement of cell death either from wild-type p53 or modified p53 combined with RT. p21 and caspase-3 protein involved in p53 pathways were evaluated in cells and tumor tissue treated with adenovirus and RT. As revealed by immunohistochemical staining, the highest expression of p21 and caspase-3 was consistent with anti-tumor effects. Each expression level was strongest for cells treated wild-type p53 and RT at low MDM2 levels and modified p53 and RT at high MDM2 levels. Western blot analysis revealed that the levels of caspase-3 and p21 were increased in the presence wild-type p53 at low MDM2 level and modified p53 at high MDM2 level, respectively. Although the mechanisms are not completely explained, the data suggest that the radiosensitization effect through apoptosis and cell cycle arrest results from modified p53 activation even with MDM2 overexpression.

The present study demonstrated that restoration of modified p53 function in MDM2-overexpessing cells was associated with an increased cell-killing effect of RT both *in vitro* and *in vivo*. However, whether this result can be applied to other tumor cells is unclear. The cell death effect of p53 status is complex and most likely dependent on many factors such as tissue-specific differences, overall genetic machinery, and complicated intracellular signaling pathways. Additionally, a p53-independent mechanism of MDM2 has been identified:[32] MDM2 promotes cell cycle progression and has a role in response to treatment, regardless of p53 status.[33] However, the present study illustrated the enhanced cell-killing effect and tumor growth delay using the combination treatment of adenovirus with RT.

In summary, the present study demonstrated that adenovirus-expressing modified p53 binding to MDM2 can effectively killing tumor cells overexpressing MDM2. Furthermore, the combination of p53-MDM2 disruption with RT showed an enhanced tumor-suppressing effect both *in vitro* and *in vivo*.

ACKNOWLEDGEMENTS

This work was supported by the Ministry of Education, Science and Technology (MEST) and the National Research

Foundation of Korea (NRF) through Nuclear R&D Program, 2010 (Grant number: 2010-0018539), a faculty research grant of Yonsei University College of Medicine for 2009 (6-2009-0102), a research fund (2008) provided from Yonsei Cancer Research Institute, and the Korea Science and Engineering Foundation (R15-2004-024-02001-0, 2009K001644, Dr. C-O. Yun). Il-Kyu Choi is a graduate student sponsored by NRF through National Core Research Center.

REFERENCES

1. Bruix J and Sherman M (2005) Management of hepatocellular carcinoma. Hepatology **42**: 1208–1236.
2. Bruix J and Sherman M (2011) Management of hepatocellular carcinoma: an update. Hepatology **53**: 1020–1022.
3. Lawrence TS, *et al* (1995) Hepatic toxicity resulting from cancer treatment. Int J Radiat Oncol Biol Phys **31**: 1237–1248.
4. Hawkins MA and Dawson LA (2006) Radiation therapy for hepatocellular carcinoma: from palliation to cure. Cancer **106**: 1653–1663.
5. Seong J (2009) Challenge and hope in radiotherapy of hepatocellular carcinoma. Yonsei Med J **50**: 601–612.
6. Gerbes AL and Caselmann WH (1993) Point mutations of the P53 gene, human hepatocellular carcinoma and aflatoxins. J Hepatol **19**: 312–315.
7. Fei P and El-Deiry WS (2003) P53 and radiation responses. Oncogene **22**: 5774–5783.
8. Picksley SM and Lane DP (1993) The p53-mdm2 autoregulatory feedback loop: a paradigm for the regulation of growth control by p53? Bioessays **15**: 689–690.
9. Chen J, Marechal V and Levine AJ (1993) Mapping of the p53 and mdm-2 interaction domains. Mol Cell Biol **13**: 4107–4114.
10. Haupt Y, *et al* (1997) Mdm2 promotes the rapid degradation of p53. Nature **387**: 296–299.
11. Vazquez A, *et al* (2008) The genetics of the p53 pathway, apoptosis and cancer therapy. Nat Rev Drug Discov **7**: 979–987.
12. Milas L, *et al* (1999) Enhancement of tumor radioresponse *in vivo* by gemcitabine. Cancer Res **59**: 107–114.
13. Nagasawa H, *et al* (1995) Relationship between radiation-induced G1 phase arrest and p53 function in human tumor cells. Cancer Res **55**: 1842–1846.
14. Vousden KH and Lu X (2002) Live or let die: the cell's response to p53. Nat Rev Cancer **2**: 594–604.
15. Kastan MB, Canman CE and Leonard CJ (1995) P53, cell cycle control and apoptosis: implications for cancer. Cancer Metastasis Rev **14**: 3–15.
16. Kastan MB, *et al* (1991) Participation of p53 protein in the cellular response to DNA damage. Cancer Res **51**: 6304–6311.
17. Roth JA, *et al* (1996) Retrovirus-mediated wild-type p53 gene transfer to tumors of patients with lung cancer. Nat Med **2**: 985–991.
18. Gotoh A, *et al* (1997) Cytotoxic effects of recombinant adenovirus p53 and cell cycle regulator genes (p21 WAF1/CIP1 and p16CDKN4) in human prostate cancers. J Urol **158**: 636–641.
19. Spitz FR, *et al* (1996) Adenoviral-mediated wild-type p53 gene expression sensitizes colorectal cancer cells to ionizing radiation. Clin Cancer Res **2**: 1665–1671.
20. Li JH, *et al* (1999) The effects of combining ionizing radiation and adenoviral p53 therapy in nasopharyngeal carcinoma. Int J Radiat Oncol Biol Phys **43**: 607–616.
21. Badie B, *et al* (1999) Combined radiation and p53 gene therapy of malignant glioma cells. Cancer Gene Ther **6**: 155–162.
22. Reifenberger G, *et al* (1993) Amplification and overexpression of the MDM2 gene in a subset of human malignant gliomas without p53 mutations. Cancer Res **53**: 2736–2739.
23. Wunder JS, *et al* (1999) Co-amplification and overexpression of CDK4, SAS and MDM2 occurs frequently in human parosteal osteosarcomas. Oncogene **18**: 783–788.
24. Barak Y, *et al* (1993) mdm2 expression is induced by wild type p53 activity. EMBO J **12**: 461–468.
25. Chen CY, *et al* (1994) Interactions between p53 and MDM2 in a mammalian cell cycle checkpoint pathway. Proc Natl Acad Sci USA **91**: 2684–2688.
26. Kussie PH, *et al* (1996) Structure of the MDM2 oncoprotein bound to the p53 tumor suppressor transactivation domain. Science **274**: 948–953.
27. Kubbutat MH, Jones SN and Vousden KH (1997) Regulation of p53 stability by Mdm2. Nature **387**: 299–303.
28. Momand J, *et al* (1992) The mdm-2 oncogene product forms a complex with the p53 protein and inhibits p53-mediated transactivation. Cell **69**: 1237–1245.
29. Shangary S and Wang S (2008) Targeting the MDM2-p53 interaction for cancer therapy. Clin Cancer Res **14**: 5318–5324.
30. Chene P (2003) Inhibiting the p53-MDM2 interaction: an important target for cancer therapy. Nat Rev Cancer **3**: 102–109.
31. Sauthoff H, *et al* (2006) Modification of the p53 transgene of a replication-competent adenovirus prevents mdm2- and E1b-55kD-mediated degradation of p53. Cancer Gene Ther **13**: 686–695.
32. Wang H, *et al* (2003) Chemosensitization and radiosensitization of human cancer by antisense anti-MDM2 oligonucleotides: *in vitro* and *in vivo* activities and mechanisms. Ann N Y Acad Sci **1002**: 217–235.
33. Zhang Z, *et al* (2004) Radiosensitization by antisense anti-MDM2 mixed-backbone oligonucleotide in *in vitro* and *in vivo* human cancer models. Clin Cancer Res **10**: 1263–1273.

Received on June 23, 2011
Revision received on September 13, 2011
Accepted on October 17, 2011